FIVE CLASSES OF CRYSTAL ARRAYS FOR BLIND DECORRELATION OF DIFFUSE NOISE

Nobutaka Ono, Nobutaka Ito, and Shigeki Sagayama

Department of Information Physics and Computing,
Graduate School of Information Science and Technology, The University of Tokyo
7-3-1 Hongo, Bunkyo-ku, Tokyo, 113-8656, JAPAN

ABSTRACT

In this paper, we mathematically discuss the sensor arrangements for decorrelating diffuse noise on channels without the knowledge of the coherence function, denoted as *blind decorrelation*, which is useful for estimating target power spectrum and designing a post filter. As a necessary condition, we show that a set of distances from the sensor i to others has to be identical for any i. Based on it, five classes of array geometries with explicit basis-transfer matrices for the decorrelation are presented.

1. INTRODUCTION

Since single or multiple target acoustic sources in real situations are occasionally interfered by diffuse noise due to many noise sources in background, reverberation, and random vibration of surrounding large surfaces like windows or walls, suppressing the diffuse noise or localizing targets in it is one of the significant topics in array signal processing. Some difficulty to handle the diffuse noise lies on the correlative nature between channels, which causes to perturb the cross correlation function in the time domain, and degrade the performance of the time delay estimation. It also distorts the eigenstructure of the covariance matrix complicatedly in the frequency domain.

The correlation is characterized by a spatial coherence function [1]. In the 3D isotropic field, it is given by a sinc function [2], which is commonly used for post-filter design [3][4] and blind source separation [5][6]. However, in some cases, it doesn't match the actual coherence function because of geometrical room shapes, reflectance difference between walls and floors, and diffraction from a rigid mount of microphones.

As another approach to deal with the diffuse noise, we have recently developed the blind decorrelation technique, which allows to decorrelate the diffuse noise, *i.e.*, clean out the isotropic noise component from cross terms of the observed covariance matrix without the explicit coherence function by arraying microphones in a special geometry like crystals. We have applied it to the estimation of the target power spectrum [7] and the design of the improved post-filter [8], but the detailed discussion for the microphone arrangement has not been presented. In this paper, focusing on it, we discuss allowable microphone arrangements for the blind decorrelation.

2. COVARIANCE MATRIX IN DIFFUSE NOISE

Let's consider that an acoustic source in the presence of diffuse noise is observed by M microphones. The observation vector in the time-frequency domain can be written as

$$\boldsymbol{O}(t,\omega) = S(t,\omega)\boldsymbol{e}(\omega) + \boldsymbol{N}(t,\omega), \tag{1}$$

where $\boldsymbol{O}(t,\omega)$ is the observation vector, $S(t,\omega)$ is the source, $\boldsymbol{e}(\omega)$ is the known steering vector, and $\boldsymbol{N}(t,\omega)$ is the diffuse noise component. For brevity, we will omit the arguments t and ω hereafter. If S and $\boldsymbol{N}$ are zero-mean and mutually uncorrelated, the covariance matrix can be written as

$$\Phi_{OO} = \phi_{SS}\boldsymbol{e}\boldsymbol{e}^H + V, \tag{2}$$

where $\Phi_{OO} = E[\boldsymbol{O}\boldsymbol{O}^H]$, $\phi_{SS} = E[|S|^2]$, and $V = E[\boldsymbol{N}\boldsymbol{N}^H]$. In the observation covariance matrix Φ_{OO}, the signal covariance matrix (the first term in the right side of eq. (2)) is corrupted by the diffuse noise term V. Our idea is to make non-diagonals of Φ_{OO} be noise-free by diagonalizing V, which has been applied for the estimation of the power spectrum ϕ_{SS} [7], and the suppression of diffuse noise [8]. It will be applied for multiple source localization. The point is how to diagonalize V, which cannot be observed.

We here assume that the diffuse noise field is spatially stationary, that is, 1) the noise power spectrum is the same on each microphone, 2) the noise cross spectrum is determined by only a distance between microphones. By normalizing diagonals to unit, the noise covariance matrix V is represented as

$$V = \begin{pmatrix} 1 & \Gamma(r_{12},\omega) & \cdots & \Gamma(r_{1n},\omega) \\ \Gamma(r_{21},\omega) & 1 & \cdots & \Gamma(r_{2n},\omega) \\ \vdots & \vdots & \ddots & \vdots \\ \Gamma(r_{n1},\omega) & \Gamma(r_{n2},\omega) & \cdots & 1 \end{pmatrix}, \tag{3}$$

where r_{ij} is the distance between the microphone i and j and $\Gamma(r,\omega)$ represents the spacial coherence function. Note that V is a symmetry matrix since $r_{ij} = r_{ji}$. Our goal here is to find microphone arrangements and corresponding unitary matrices U such that $U^H V U$ is constantly diagonal for any coherence function $\Gamma(r,\omega)$.

3. CRYSTAL ARRAYS

3.1. Necessary Condition

First, we begin with the following lemma.

Lemma 1 *A necessary condition for V defined by eq. (3) to be diagonalize by an unitary matrix U for any function $\Gamma(r,\omega)$, is that a set of distances from the sensor i to others: $\{r_{i1}, r_{i2}, \cdots, r_{in}\}$ is identical for any i.*

Proof: If V is diagonalized by an unitary matrix U without dependence on $\Gamma(r,\omega)$, the matrix I_n, of which all elements are identical to 1, is also diagonalized by U since I_n is obtained by letting $\Gamma(r,\omega) = 1$. Then, V and I_n are commutative. From (i,j) element of $VI_n = I_nV$, we see that

$$\sum_{k=1}^{n} \Gamma(\omega, r_{ik}) = \sum_{k=1}^{n} \Gamma(\omega, r_{jk}) \tag{4}$$

has to be an identical equation of r_{ij}s. It means that a distance set: $\{r_{ij} |\, j = 1, 2, \cdots n\}$ must be identical for any i. ■

Lemma 1 shows that, at least, all sensors must be on a sphere because the distance between the sensor i and the center, defined by $\boldsymbol{r}_0 = \sum_j \boldsymbol{r}_j / N$ where $\boldsymbol{r}_j$ represents the jth sensor position, is calculated as $r_{i0} = \sqrt{|\boldsymbol{r}_i - \boldsymbol{r}_0|^2} = \sqrt{\sum_j r_{ij}^2}/N$, which is identical for any i. Furthermore, there should exist permutations of sensors to invariantly maintain the array structure. We currently conjecture that it is deeply related to the group theory in mathematics, especially, *a point group*, which is the group of the geometrical operations to leave the origin fixed like rotations, mirror reflections, etc [9]. Indeed, from their groups, we have obtained five classes of point sets satisfying Lemma 1. For example, the rotations of $2\pi i/n$ $(i = 1, 2, \cdots, n)$ in xy plane, the reflection about z plane, and their combinations form a kind of the point group. Moving a point by their operations yields a regular polygonal prism arrangement. Although the connection of the group theory to the blind decorrelation has not been rigorous yet, here we can show the sufficiency of their arrays for the blind decorrelation by deriving U such that $U^H V U$ is diagonal. From the analogy to the fact that possible crystal structures are provided from the group theory in crystallography, we call them *crystal arrays*.

3.2. Five classes of crystal arrays

1) Regular polygons

Let *circ* denote a circulant matrix as

$$\mathrm{circ}(1, a, b) = \begin{pmatrix} 1 & a & b \\ b & 1 & a \\ a & b & 1 \end{pmatrix}. \tag{5}$$

In arraying sensors on vertices of a n-sided regular polygon, circularly numbering them as shown in Fig. 1(a) yields a circulant $V = \mathrm{circ}(1\ a_1\ a_2 \cdots\ a_2\ a_1)$. As well known, it is diagonalized by n-th order DFT matrix Z_n [10].

2) Rectangular

The second class consists of only a rectangular. Under numbering sensors as shown in Fig. 1(b), V has a block-circulant structure as

$$V = \begin{pmatrix} F_1 & F_2 \\ F_2 & F_1 \end{pmatrix}, \tag{6}$$

where F_1 and F_2 are 2×2 circulant matrices. It is diagonalized by $U = Z_2 \otimes Z_2$.

3) Regular polygonal prisms

The regular polygonal prism arrangement is given by merging vertices of two parallel n-sided polygons with the same center axis. As the rectangular case, V has a block-circulant structure as

$$V = \begin{pmatrix} F_1 & F_2 \\ F_2 & F_1 \end{pmatrix}, \tag{7}$$

where F_1 and F_2 are $n \times n$ circulant matrices. It is diagonalized by

$$U = Z_n \otimes Z_2 = \begin{pmatrix} Z_n & Z_n \\ Z_n & -Z_n \end{pmatrix}. \tag{8}$$

The two parallel n-sided polygon may have a certain different angle, which yields a twisted prism as shown in Fig. 1(c). In $n = 2$, any angles are allowable, which the matrix structure is invariant for. In $n \geq 3$, only the rotation with π/n is allowable, where V becomes simply circular by alternative numbering in the top and the bottom n-sided polygon as shown in Fig. 1(c).

4) Rectangular solid

In related to a rectangular, a rectangular solid forms another class. By numbering sensors shown in Fig. 1(d), V has the following structure:

$$V = \begin{pmatrix} F_1 & F_2 & F_3 & F_4 \\ F_2 & F_1 & F_4 & F_3 \\ F_3 & F_4 & F_1 & F_2 \\ F_4 & F_3 & F_2 & F_1 \end{pmatrix}, \tag{9}$$

where F_i $(i = 1, 2, 3, 4)$ are 2×2 circulant matrices. V itself is not circulant but it has recursively circulant structure. Hence, it is diagonalized by $U = Z_2 \otimes Z_2 \otimes Z_2$.

5) Regular polyhedrons

As well known, there are only five polyhedrons in a 3D space: tetrahedron, octahedron, hexahedron, icosahedron, and dodecahedron, and they form the last class. From the viewpoint of the covariance matrix form, the tetrahedron is a special case of a twisted 2-sided polygonal prism, while the octahedron and the hexahedron are a special case of twisted 3-sided and 4-sided polygonal prisms, respectively. The most difficult cases are given by the icosahedron and the dodecahedron arrangements.

An icosahedron has twenty equilateral triangular faces. Let two opposed triangulars be the top and the bottom faces. Then, all vertices lie in four parallel planes. Numbering vertices circularly in the top plane, and then, from the top to the bottom in order as shown in Fig. 1(e), we have

$$V = \begin{pmatrix} F_1 & F_2 & F_3 & F_4 \\ F_2 & F_5 & F_6 & F_3 \\ F_3 & F_6 & F_5 & F_2 \\ F_4 & F_3 & F_2 & F_1 \end{pmatrix}, \tag{10}$$

$$\begin{aligned} F_1 &= \mathrm{circ}(1\ a\ a), \quad F_2 = \mathrm{circ}(b\ a\ a), & (11)\\ F_3 &= \mathrm{circ}(a\ b\ b), \quad F_4 = \mathrm{circ}(c\ b\ b), & (12)\\ F_5 &= \mathrm{circ}(1\ b\ b), \quad F_6 = \mathrm{circ}(c\ a\ a). & (13) \end{aligned}$$

Unlike the other cases, V doesn't have the circulant structure. Taking into consideration that 1) F_i $(1 \le i \le 6)$ is diagonalized by Z_3 (the 3rd order DFT matrix) and 2) the block structure is different between the first, fourth columns and the second, third columns, we assume that U has the following form:

$$U = \begin{pmatrix} Z_3 & Z_3 & Z_3 & Z_3 \\ Z_3P_3 & Z_3Q_3 & -Z_3R_3 & -Z_3S_3 \\ Z_3P_3 & Z_3Q_3 & Z_3R_3 & Z_3S_3 \\ Z_3 & Z_3 & -Z_3 & -Z_3 \end{pmatrix}, \tag{14}$$

where P_3, Q_3, R_3, and S_3 are diagonal matrices. Eq. (14) yields

$$Z^HVZ = \begin{pmatrix} K_1 & A & O & O \\ A & K_2 & O & O \\ O & O & K_3 & B \\ O & O & B & K_4 \end{pmatrix}, \tag{15}$$

where K_i $(1 \le i \le 4)$ are diagonal matrices with the size of 3×3 and

$$\begin{aligned} A &= (G_1 + G_2Q_3 + G_3Q_3 + G_4) \\ &\quad + P_3(G_2 + G_5Q_3 + G_6Q_3 + G_3) \\ &\quad + P_3(G_3 + G_6Q_3 + G_5Q_3 + G_2) \\ &\quad + (G_4 + G_3Q_3 + G_2Q_3 + G_1), & (16)\\ B &= (G_1 - G_2S_3 + G_3S_3 - G_4) \\ &\quad - R_3(G_2 - G_5S_3 + G_6S_3 - G_3) \\ &\quad + R_3(G_3 - G_6S_3 + G_5S_3 - G_2) \\ &\quad - (G_4 - G_3S_3 + G_2S_3 - G_1), & (17) \end{aligned}$$

$$\begin{aligned} G_1 &= \mathrm{diag}(1+2a\ \ 1-a\ \ 1-a), & (18)\\ G_2 &= \mathrm{diag}(2a+b\ \ b-a\ \ b-a), & (19)\\ G_3 &= \mathrm{diag}(a+2b\ \ a-b\ \ a-b), & (20)\\ G_4 &= \mathrm{diag}(2b+c\ \ c-b\ \ c-b), & (21)\\ G_5 &= \mathrm{diag}(1+2b\ \ 1-b\ \ 1-b), & (22)\\ G_6 &= \mathrm{diag}(2a+c\ \ c-a\ \ c-a), & (23) \end{aligned}$$

where *diag* denote a diagonal matrix as

$$\mathrm{diag}(a,b,c) = \begin{pmatrix} a & 0 & 0 \\ 0 & b & 0 \\ 0 & 0 & c \end{pmatrix}. \tag{24}$$

From A=0 for any $ab$and c, we can find a solution as

$$\begin{aligned} p_1 &= p_2 = p_3 = 1, & (25)\\ q_1 &= q_2 = q_3 = -1, & (26) \end{aligned}$$

where p_i and q_i $(i = 1,2,3)$ are diagonal components of P_3 and Q_3, respectively. In the same way, from $B = 0$, we obtain

$$\begin{aligned} r_1 = \gamma_+^2 + \gamma_+, &\quad s_1 = \gamma_-^2 + \gamma_-, & (27)\\ r_2 = r_3 = \gamma_+, &\quad s_2 = s_3 = \gamma_-, & (28) \end{aligned}$$

where r_i and s_i $(i = 1,2,3)$ are diagonal components of R_3 and S_3, respectively, and

$$\gamma_+ = (1+\sqrt{5})/2, \quad \gamma_- = (1-\sqrt{5})/2. \tag{29}$$

Consequently,

$$\begin{aligned} P_3 &= \mathrm{diag}(1\ 1\ 1), & (30)\\ Q_3 &= -\mathrm{diag}(1\ 1\ 1), & (31)\\ R_3 &= \mathrm{diag}(\gamma_+^2 + \gamma_+\ \ \gamma_+\ \ \gamma_+), & (32)\\ S_3 &= \mathrm{diag}(\gamma_-^2 + \gamma_-\ \ \gamma_-\ \ \gamma_-), & (33) \end{aligned}$$

in eq. (14) gives us U to diagonalize eq. (10).

By the similar numbering to the icosahedron shown in Fig. 1(e), V in the dodecahedron has the same block structure as eq. (10) where

$$\begin{aligned} F_1 &= \mathrm{circ}(1\ a\ b\ b\ a), \quad F_2 = \mathrm{circ}(a\ b\ c\ c\ b), & (34)\\ F_3 &= \mathrm{circ}(d\ c\ b\ b\ c), \quad F_4 = \mathrm{circ}(e\ d\ c\ c\ d), & (35)\\ F_5 &= \mathrm{circ}(1\ b\ d\ d\ b), \quad F_6 = \mathrm{circ}(e\ c\ a\ a\ c). & (36) \end{aligned}$$

The form of U is also the same structure as eq. (14), just replacing the subscript *3* by *5*, where

$$\begin{aligned} P_5 &= \mathrm{diag}(1\ \ \gamma_-^2\ \ \gamma_+^2\ \ \gamma_+^2\ \ \gamma_-^2), & (37)\\ Q_5 &= -\mathrm{diag}(1\ \ \gamma_+^2\ \ \gamma_-^2\ \ \gamma_-^2\ \ \gamma_+^2), & (38)\\ R_5 &= \mathrm{diag}(\gamma_+^2 + \gamma_+\ \ \gamma_+\ \ \gamma_+\ \ \gamma_+\ \ \gamma_+), & (39)\\ S_5 &= \mathrm{diag}(\gamma_-^2 + \gamma_-\ \ \gamma_-\ \ \gamma_-\ \ \gamma_-\ \ \gamma_-). & (40) \end{aligned}$$

4. CONCLUSIONS

In this paper, we discussed geometrical sensor arrangements, for the blind decorrelation of diffuse noise, denoted as crystal arrays. With a necessary condition, we showed explicit five classes: 1) regular polygons, 2) rectangular, 3) regular polygonal prisms, 4) rectangular solid, and 5) polyhedrons, the first two of which have two dimensional, and other three have three dimensional geometries, respectively. With clarifying the presence or the absence of other crystal arrays, combining the blind decorrelation technique with MUSIC (MUltiple Signal Classification) is our current concern.

5. ACKNOWLEDGMENT

The authors specially thank to Prof. Kazuo Murota for the discussion about the group theory, Mr. Hitoshi Kohno for Lemma 1, and the three reviewers for thoughtful comments.

6. REFERENCES

[1] M. Brandstein, D. Ward, *Microphone arrays*, Springer-Verlag, 2001.

[2] R. K. Cook, R. V. Waterhouse, R. D. Berendt, S. Edelmann and M. C. Thompson, “Measurement of correlation coefficients in reverberant sound fields,” *J. Acoust. Soc. Amer.*, vol. 27, no. 6, pp. 1072-1077, 1955.

[3] I. A. McCowan and H. Bourlard, “Microphone Array Post-Filter Based on Noise Field Coherence,” *IEEE Trans. Acoustic, Speech, and Audio Processing*, vol. 11, no. 6, Nov. 2003.

[4] S. Lefkimmiatis and P. Maragos, “A generalized estimation approach for linear and nonlinear microphone array post-filters,” *Speech Commun.*, vol. 49, pp. 657–666, 2007.

[5] R. Balan, J. Rosca, and S. Rickard, “Non-square BSS under coherent noise by beamforming and time-frequency masking,” *Proc.ICA 2003*, Nara, Apr. 2003.

[6] Y. Izumi, N. Ono, and S. Sagayama, “Sparseness-based 2ch BSS using the EM Algorithm in Reverberant Environment,” *Proc. WASPAA*, pp.147-150, Oct. 2007.

[7] H. Shimizu, N. Ono, K. Matsumoto, and S. Sagayama, “Isotropic noise suppression on power spectrum domain by symmetric microphone array,” *Proc. WASPAA*, pp. 54–57. Oct. 2007.

[8] N. Ito, N. Ono, and S. Sagayama, “A blind noise decorrelation approach with crystal arrays on designing post-filters for diffuse noise suppression,” *Proc. ICASSP*, pp. 317–320, Mar. 2008.

[9] S. Sternberg, *Group theory and physics*, Cambridge University Press, 1994.

[10] G. Golub and C. Van Loan, *Matrix computations*, Johns Hopkins University Press, 1996.

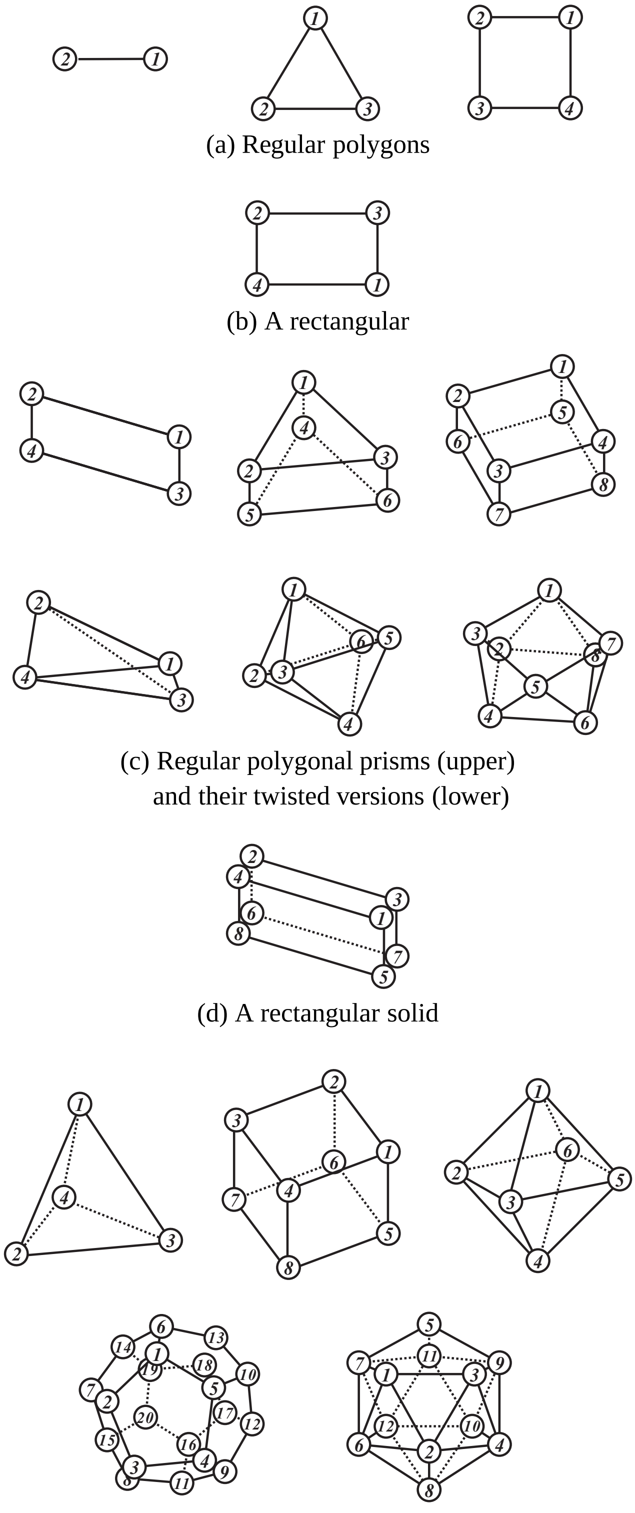

Fig. 1. Five classes of crystal arrays and examples of numbering sensors